Characterization of the Glu and Asp Residues in the Active Site of Human β-Hexosaminidase B†

Yongmin Hou,‡ David J. Vocadlo,§ Amy Leung,‡ Stephen G. Withers,§ and Don Mahuran*,‡

The Research Institute, The Hospital for Sick Children, Toronto, Ontario M5G 1X8 and the Department of Laboratory Medicine and Pathobiology, University of Toronto, Toronto, Ontario M5G 2C4, Canada, and Department of Chemistry, University of British Columbia, Vancouver, British Columbia V6T 1Z1, Canada

Received August 25, 2000; Revised Manuscript Received November 24, 2000

ABSTRACT: Human β-hexosaminidase A ($\alpha\beta$) and B ($\beta\beta$) are composed of subunits (α and β) that are 60% identical and have been grouped with other evolutionarily related glycosidases into "Family 20". The three-dimensional structure of only one Family 20 member has been elucidated, a bacterial chitobiase. This enzyme shares primary structure homology with both the human subunits only in its active-site region, and even in this restricted area, the level of identity is only 26%. Thus, the validity of the molecular model for the active site of the human enzyme based on chitobiase must be determined experimentally. In this report, we analyze highly purified mutant forms of human hexosaminidase B that have had conservative substitutions made at Glu and Asp residues predicted by the chitobiase model to be part of its active site. Mutation of βGlu^{355} to Gln reduces k_{cat} 5000-fold with only a small effect on K_m, while also shifting the pH optimum. These effects are consistent with assignment of this residue as the acid/base catalytic residue. Similarly, mutation of βAsp^{354} to Asn reduced k_{cat} 2000-fold while leaving K_m essentially unaltered, consistent with assignment of this residue as the residue that interacts with the substrate acetamide group to promote its attack on the anomeric center. These data in conjunction with the mutagenesis studies of Asp^{241} and Glu^{491} indicate that the molecular model is substantially accurate in its identification of catalytically important residues.

There are two major β hexosaminidase (Hex)[1] isozymes in normal human tissues, Hex A ($\alpha\beta$) and Hex B ($\beta\beta$). A very small amount of a third unstable isozyme, Hex S ($\alpha\alpha$), can be detected in cells that are deficient in the β protein, i.e., from Sandhoff patients. The primary structures of the α and β subunits are 60% identical. Thus, they must also share very similar three-dimensional structures with conserved functional domains. Despite data showing that monomeric subunits are not active, the existence of the three Hex isozymes, representing all possible dimeric combinations of α and/or β subunits, indicates that each subunit must contain all the residues necessary to form an active site. While all three Hex isozymes can cleave the terminal nonreducing β1−4 linked glycosidic bonds of either amino sugar (GlcNAc or GalNAc), e.g., from Asn-linked oligosaccharides or some neutral glycolipids, only Hex A and Hex S can cleave terminal nonreducing GlcNAc-6-sulfate residues in keratan sulfate, and only Hex A can cleave the GalNAc residue from GM2 ganglioside. Sensitive, fluorescent, artificial substrates have been developed that mimic the former two groups of natural substrates, 4-methylumbelliferyl 2-acetamido-2-deoxy-β-D-glucopyranoside (MUG, total Hex) and 2-acetamido-2-deoxy-β-D-glucopyranoside-6-sulfate (MUGS, Hex A and Hex S). Although MUGS is often referred to as α-specific, the β-active site can also slowly hydrolyze this substrate. The MUG:MUGS ratio for each isozyme is Hex B, 300:1; Hex A, 4:1; and Hex S, 1:1 (*1*). GM2 ganglioside is a novel substrate which is truly Hex A-specific, primarily because the isozyme must also properly interact with the small GM2 activator protein which serves as a substrate specific cofactor for Hex A in this reaction (reviewed in ref *2*). Thus, in vivo, it is the GM2 activator:GM2 ganglioside complex that is the true Hex A-specific substrate. It follows that defects in any of the genes encoding the subunits of Hex A (*HEXA* encodes α, and *HEXB* encodes β) or the monomeric GM2 activator (*GM2A*) can result in the lysosomal accumulation of GM2 ganglioside, mainly in neuronal tissues where its synthesis is greatest, causing inheritable neurodegenerative diseases, collectively known as the G_{M2} gangliosidoses: Tay-Sachs, *HEXA* mutations; Sandhoff disease, *HEXB* mutations; and AB-variant, *GM2A* mutations (reviewed in refs *3* and *4*).

Human Hex A and B are also models for other Family 20 glycosidase (*5*). Members of this family are believed to be evolutionarily and, thus, structurally related. These enzymes are now believed to work through an acid−base-catalyzed

† This work was supported by a Canadian Institutes of Health Research grant to D.M.

* To whom correspondence should be addressed. Phone: (416) 813-6161. Fax: (416) 813-8700. E-mail: hex@sickkids.on.ca.

‡ University of Toronto.

§ University of British Columbia.

[1] Abbreviations: Hex, β-hexosaminidase; G_{M2}, G_{M2} ganglioside, GalNAcβ(1−4)-[NANAα(2−3)-]-Galβ(1−4)-Glc-ceramide; MU, 4-methylumbelliferone; MUG, 4-methylumbelliferyl-β-*N*-acetylglucosaminide; MUGS, 4-methylumbelliferyl-β-*N*-acetylglucosaminide-6-sulfate; CNAG, 2-acetamido-*N*-(ϵ-aminocaproyl)-2-deoxy-β-D-glucopyranosylaminide; ER, endoplasmic reticulum; CRM, cross-reacting material; δ-lactone, 2-acetamido-2-deoxy-D-glucono-1,5-lactone; NTA, nitrilotriacetic acid; FCS, fetal calf serum.

10.1021/bi002018s CCC: $20.00
Published on Web 01/23/2001

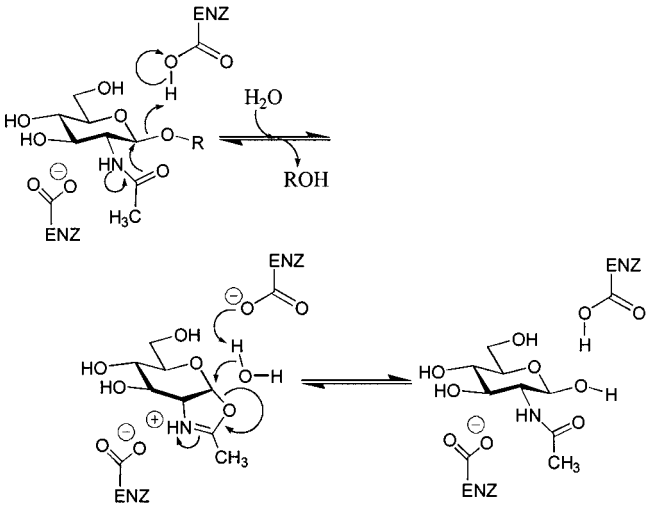

FIGURE 1: Proposed mechanism of human β-hexosaminidases and other family 20 β-hexosaminidases and chitobiases.

mechanism (Figure 1) in which the *N*-acetyl substituent of the substrate functions as an intramolecular nucleophile to form an oxazolinium-ion intermediate. Whether this enzyme-bound intermediate is the protonated oxazolinium ion or a neutral oxazoline remains unknown. An acid catalyst in the active site assists by protonating the glycosidic oxygen while another carboxyl group acts to stabilize the transition state leading to the formation of an oxazolinium-ion intermediate. Hydrolysis of this intermediate occurs via attack of water at the anomeric center with general base catalysis from the same group that originally acted as the acid catalyst (*6*, *7*). Data from the crystal structure of a chitobiase−substrate complex from Family 20, supports this mechanism (*8*).

Since all the members of a given hydrolase family are believed to have similar three-dimensional structures, molecular modeling of human Hex and recently Hex from *Streptomyces plicatus*, Sp-Hex, has been tried based on the known structure of chitobiase. The overall three-dimensional structure that was generated for monomeric Sp-Hex (*9*) was similar to the previously reported model for the human α subunit of Hex A (*8*). However, the related monomeric bacterial chitobiase has only 26% sequence identity to its human counterpart, and this occurs only within their active-site regions. Outside of this region, there is little sequence similarity. As well, the Sp-Hex has only 25% sequence identity to human Hex (*9*). Thus, the modeling data for the active sites of the human Hex subunits need to be validated experimentally.

Previous hopes of identifying structure−function relationships in human Hex through analysis of mutations associated with GM2 gangliosidoses have not been realized because most naturally occurring mutations, even missense mutations, first affect protein-transport out of the endoplasmic reticulum (ER) (reviewed in refs *4* and *10*). Thus, disease-causing missense mutations in either the *HEXA* or *HEXB* genes can result in a Hex A with an unaltered specific activity, but with its total protein level reduced to between 0 and 10% of normal.

The missense mutations associated with the B1-variant of Tay-Sachs disease behave differently than the transport-impaired mutations describe above. In these cases, patients have near normal levels of Hex A protein and MUG activity, but hydrolysis of MUGS or the GM2 ganglioside:GM2 activator complex by the isozyme can no longer be detected (*11*). Thus, it was postulated that the corresponding mutation may affect an active-site residue. The classic missense mutation associated with this phenotype is αArg^{178}His (*12*). In keeping with the hypothesis that structure−function relationships are conserved between the α and β subunits, when we analyzed the mutation in the aligned codon in the β subunit, βArg^{211}His, we found that it produced near normal levels of dimeric Hex B that was virtually devoid of MUG activity (*13*). This observation remained true even when Lys was substituted for βArg^{211} (*14*). Thus, the quality control system in the ER is very sensitive to any change in the folding patterns caused by mutations to the proteins occurring in its lumen. However, some mutations that are conservative substitutions and affect active-site residues are able to bypass this system and be delivered to the lysosome (reviewed in refs *4* and *10*).

To test candidate active-site residues identified from the chitobiase model, in vitro mutagenesis, protein expression and purification, and kinetic analyses must be performed. In the case of proteins such as Hex that are synthesized in the ER, mammalian or insect cells have been used. Bacterial expression of Hex produces only inactive protein that cannot be refolded into a functional form (unpublished data). One advantage of mammalian cell expression is the ability to easily identify those mutations that have had additional effects on the folding of the Hex subunits through their increased retention in the ER. Such a system also exists in insect cells although it appears not to be as stringent. The major disadvantage to either system is that both cell types contain endogenous Hex which, depending on the down stream purification method used, leads to a reduced signal (from human Hex) to noise (from endogenous Hex) ratio. A large signal-to-noise ratio is particularly important when analyzing candidate active-site residues. For example, neutralization of the catalytic acid group can be expected to reduce k_{cat} by >1000-fold with only a small effect on K_m (often a small decrease) (*15*). Therefore, an expression system that results in a signal-to-noise ratio of ≪1000 cannot distinguish between the catalytic acid residue and a group more indirectly involved in catalysis.

All of the previous analyses of the active site of human Hex using in vitro mutagenesis and cellular expression encountered the problem of endogenous Hex contamination (signal:noise < 100) (*16*, *17*). Thus, no absolute conclusion has been reached as to the validity of the model of human Hex based on the structure of chitobiase. To resolve this issue, we have recently developed a method that generates a tagged form of human Hex B that can be purified away from all endogenous Hex (*18*). We introduced a sequence that encodes a factor X site and His_6 sequence at the 3′ end of the βcDNA, which we then permanently transfect into CHO cells. We found that the His_6-tagged pro-Hex B is not retained in the ER, but is either transported to the lysosome or secreted; however, the tag is lost once the protein enters the lysosome. We demonstrated that pro-Hex B−His_6 can be purified directly from the medium of the transfected cells using Ni-NTA chromatography under native conditions with a signal-to-noise ratio of ∼50000:1. We further demonstrated that this purified pro-Hex B−His_6 has identical biochemical properties to the mature, lysosomal form. Using this highly purified form of Hex B, we initially tested the validity of

Table 1: Residues Involved in the Active Site of Chitobiase and Their Aligned Residues in Streptomyces Plicatus Hex and Human Hex, α and β Subunits

Sp-Hex	Sp-Hex experimental data (*9*)	c-#	function predicted in chitobiase (*8*)	α#	β#	human Hex experimental data
D147		D334	no function postulated	D163	D196[a]	βD196N: precursor but no mature β-CRM[b]
D159		D346	holds R349 in place by polar interaction, H-bonds to term. amino and imino groups	D175	D208	βD208N: monomeric precursor but no mature β-CRM (*19*); protein trapped in the ER (*22*)
R162	R162His: K_m (0.14 mM, MUG) increased by 40-fold, V_{max} reduced 5-fold	R349	docks the GlcNAc by H-binding at OH3 and OH4, sits at the base of the binding pocket	R178(B1)	R211[a]	βR211K: mature β-CRM; K_m increased >10-fold, 0.2% k_{cat} (*18*)
D191		D378	holds R349 in place by polar interaction, H-bonds to H452	D207	D240	βD240N: mature β-CRM, K_m increased 10-fold, k_{cat} = 10% (*19*)
D192		D379	holds R349 in place by polar interaction, coordinates water mol with E380	D208	D241[a]	D241N: mature β-CRM, K_m increased 3-fold, k_{cat} = 5%
D246	D246N: K_m increased 1.2-fold, V_{max} decreased 2-fold	D448	H-bonds to D539, indirectly H-bonds substrate through a H_2O mol	D258	D290	D290N: 20-fold reduction in mature β-CRM; K_m increased 3-fold, k_{cat} = 70% (*19*)
D313		D539	H-bonds to acetamido-N to help distort it toward C1 and stabilize oxazolinium-ion intermediate	D322	D354[a]	mature β-CRM, normal K_m, k_{cat} = 0.04%
E314	E314Q: K_m decreased 7-fold, V_{max} decreased 296-fold altered pH profile	E540	binds glycosidic oxygen, catalytic acid	E323	E355[a]	βE355: Identified by photoaffinity label (*31*); αE323 and βE355: implicated as an active residue by expression studies (*16*, *17*). [a]βE355Q: mature β-CRM, slightly reduced K_m, k_{cat} = 0.02%
442W		E739	H-bonds incoming H_2O molecule, H-bonds between OH5B	E462	E491[a]	E491Q: mature β-CRM, normal K_m and V_{max}

[a] Residues tested by expression in CHO cells of Asp→Asn or Glu→Gln substituted pro-Hex B−His_6 which was purified by Ni^{2+} chromatography (Figure 3). Each mutation was confirmed to have produced mature β-CRM in transfected cell lysates (Figure 2). [b] Previous findings of normal levels of mature $Asp^{196}Asn$ substituted β-protein in transfected cell lysates were incorrect (*19*).

the molecular modeling of human Hex from the chitobiase structure by reexamining the effect of the $\beta Arg^{211}Lys$ substitution. The K_m (~10-fold increase) and k_{cat} (~0.2% of wild-type) values of the mutant protein for the hydrolysis of MUG and its ability to bind the affinity ligand CNAG (reduced by ~10-fold) were determined. These data demonstrated that, in agreement with the chitobiase model, βArg^{211} has a major role in substrate binding. However, it also has a role in catalysis which was not predicted from the model but is consistent with our previous biochemical data (*14*). Our previous data incorrectly indicated a normal K_m for this mutant protein, which we now know was the result of a small amount of contaminating CHO cell Hex coupled with the severely reduced k_{cat} of the mutant (*18*).

In this report, we extend our investigation of the validity of the chitobiase model by examining other candidate active-site residues in Hex B. We analyzed the role of the acidic residues that are conserved in human Hex and have been identified as active residues in bacterial chitobiase, in part using our new C-terminal His_6-tag methodology. Kinetic analysis of these purified mutant proteins from the transfected CHO cells, followed by CNAG affinity binding assays demonstrates that much of the chitobiase model of human Hex is valid.

MATERIALS AND METHODS

Protein Homology Alignment and Modeling. Sequence alignment of the catalytic domain of chitobiase, Sp-Hex, and human Hex α and β subunits was made based on a molecular modeling system that uses secondary structure predictions to calculate gaps (*8*, *9*). The alignment covers only the active-site area of the enzymes since there is little similarity in the sequences outside of this region. Candidate acidic residues involved in the active site of human Hex are shown in Table 1.

Site-Directed Mutagenesis and Vector Construction. The mutations were made in plasmid pHexB43 (*13*). The construction of βcDNA encoding an Asp196Asn substitution was previously reported (*19*). However, its correct sequence was reconfirmed for this study. For all other mutations (Table 2), mutagenesis was performed by a two-step PCR procedure (*20*), which involved the utilization of three different oligonucleotides. Briefly, in step 1, amplification was achieved by an oligo containing the appropriate nucleotide change (Table 2) and a 3′ end oligo. This PCR product (termed "intermediate") containing the point mutation of interest then served as a "mega-primer" in conjunction with the 5′ end oligo to yield the final product of the second round

Table 2: Oligonucleotides Used to Mutate βcDNA[a]

no.	oligonucleotides	change	substitution induced
1	5′-TCCACCATTATTAAC[a]TCTCCAAGGGTTT-3′	GAT6AAC	Asp196Asn
2	5′-GGCACATAGTTGATAACCAGTCTT-3′	GAC6AAC	Asp241Asn
3	5′-TTTGGGAGGAAATGAAGTGGAATT-3′	GAT6AAT	Asp354Asn
4	5′-TTTGGGAGGAGATCAAGTGGAATT-3′	GAA6CAA	Glu355Gln
5	5′-ATGGGGACAATATGTGGATGCAAC-3′	GAA6CAA	Glu491Gln
6	5′-AGATAGTGTATGCCCAGGGGTAT-3′	3′ primer[b]	none
7	5′-GGTTTCTACAAGTGGCATCAT-3′	5′ primer[b]	none
8	5′-CCTCCAATCTTGTCCATAGCTA-3′	3′ primer	none
9	5′-CCAAATGATGTCCGTATGGTGATT-3′	5′ primer	none
10	5′-TGGTTTGTCCAAACTCATCAATGTA-3	3′ primer	none
11	5′-GGTTTTGGATATTATTGCAACCATAA-3′	5′ primer	none

[a] The nucleotide changes are underlined, and the changes consequently made in the deduced amino acid sequence of the β-subunit are also shown. [b] Oligos 6 and 7 serve as the 5′ and 3′ end primers to create the Asp[241]Asn substitution by the two-step PCR procedure; whereas oligos 10 and 11 are utilized for generation of the Glu[491]Gln substitution (see text). The 5′ and 3′ end primers used for generation of either the Asp[354]Asn or Glu[355]Gln mutation are oligos 8 and 9. All these primers contain proper restriction enzyme sites for facilitation of subcloning the PCR fragment back into the pHEXB43 (see details in Materials and Methods).

PCR reaction. The 5′ and 3′ end oligonucleotides each carry proper restriction sites to facilitate the ligation of the final PCR product containing the derived mutation into pHexB43. To remove any contamination of the residual oligonucleotides used in step 1 of the reaction, the intermediate product (generated from step 1) was purified using the Geneclean kit (Bio 101 Inc., Vista, CA) before it was used for the step 2 amplification. Amplifications were achieved using Vent polymerase (BioLabs Inc., Beverly, MA) to increase the fidelity. The reactions were carried out in 100 μL volumes. Each reaction mix contained 50 ng of DNA template, 20 mM Tris-HCl (pH 8.8), 10 mM KCl, 10 mM $(NH_4)_2SO_4$, 2 mM $MgSO_4$, 0.1% Triton X-100, 0.2 mM each of dNTPs, 100 ng of each oligo, and 2 units of Vent DNA polymerase (BioLabs Inc.). The cycling steps used were as follows: one cycle of heat denaturation at 95 °C for 5 min, 28 cycles each consisting of denaturation at 95 °C for 30 s, annealing at 56 °C for 1 min, and extension at 73 °C for 1 min, and one cycle of 73 °C for 7 min, in a Perkin-Elmer-Cetus thermal cycler 2400. Generation of the Asp[241]Asn substitution included the following procedure: (a) first round of amplification of the 260 bp DNA fragment using oligos 2 and 6 (Table 2); (b) second round of amplification of the 669 bp fragment using the 260 bp intermediate product and oligo 7 (Table 2); (c) digestion of the 669 bp DNA with *Eco*R1 and subcloning it into pHEXB43 to replace the corresponding wild-type segment. Similarly, a 582 bp EcoR1−Bsu36 I DNA fragment containing a Asp[354]Asn or Glu[355]Gln mutation was generated by two-step PCR using oligos 3, 8, and 9 or oligos 4, 8, and 9, respectively. Subsequently, either of the above fragments was ligated into pHEXB43 that was treated by *Bsu*36I and partial *Eco*R1 digestion. To create Glu[491]Gln substitution, oligos 5, 10, and 11 were utilized to amplify a 715 bp *Bam*H1 DNA fragment. All the mutant cDNA inserts in pHEXB43 were fully sequenced and verified by T7 sequencing kit (Pharmacia). Next, the 1.5 kb *Bst*XI inserts, each containing a substitution described above, were subcloned into pcDNA-β-His_6 (*18*) to replace its corresponding segment. The mutation (indicated by β*) and orientation of the insert in the resulting pcDNA-β*-His_6 were reverified by DNA sequencing before transfection of the DNA into CHO cells.

Transfection of Mutant Constructs. CHO cells were maintained and propagated in α-MEM supplemented with 10% FCS and antibiotics at 37 °C in 5% CO_2. Transfections were carried out using Superfect Reagent (Qiagen, Valencia, CA), as described (*18*). Neomycin (400 μg/mL) was present in all the stable transfectants. Since no significantly increased level of Hex activity was detected in the media of some cells transfected with mutant constructs, Western blot analysis was used to assess their level of cellular expression.

Assays of Enzyme and Protein Levels. Harvested cells were lysed in a buffer of 10 mM Tris-HCl (pH 7.5) and 5% glycerol through five sets of freeze−thaw cycles. Protein concentrations were measured by the Lowry method (*21*). Human Hex activities from the cells' lysates and media were determined using the MUG substrate (*13*). Western blotting was done essentially as described previously (*22*). The primary and secondary antibodies used were a rabbit anti-human Hex A (*20*, *23*) and a horseradish peroxidase-conjugated goat anti-rabbit IgG (Immux), respectively. The nitrocellulose membrane containing the proteins was developed and exposed to Hyperfilm using the ECL system (Amersham).

Purification of His_6-Tagged Mutant Hex B Protein. Ten plates (Falcon P150) of transfected CHO cells were initially subcultured in αMEM medium containing10% FCS. When the cells were 80% confluent, the plates were washed twice with 20 mL of PBS and the media changed to CHO SFMII (GIBCO). After 4 days, the medium was collected from each plate and replaced with another 20 mL of CHO SFMII medium. This procedure was repeated twice more. The media was then pooled and centrifuged at 3000 rpm, and the pellet discarded. The cleared media (650 mL) was concentrated to 150 mL with hollow fiber concentrator (AMICON, 10 kDa cut off). The concentrated medium was then dialyzed against QIAGEN lysis buffer (20 mM imidazole, 500 mM NaCL, 50 mM NaH_2PO_4, 1% Tween 20, and 10% glycerol, pH 8.0). It was then transferred into a Falcon tube containing 800 μL of QIAGEN Ni-NTA resin, and rotated at 4 °C overnight. The resin was next packed into a column which was washed with 20 mL QIAGEN lysis buffer. The column was then washed with 10 mL of 100 mM imidazole in lysis buffer. Human Hex was specifically eluted with 250 mM imidazole in lysis buffer. Ten 1 mL fractions were collected and assayed for protein and Hex activity. The fractions containing protein and detectable Hex activity were concentrated and the buffer exchanged for 10 mM phosphate buffer pH 6.0, using Centriplus concentrators (AMICON).

Kinetic Studies. The concentration of MUG substrate used in each assay was varied from 0.1 to 4 mM for the determination of the K_m and V_{max} values. Because of the limited solubility of MUG, 4 mM represents the near maximum concentration of substrate achievable. The kinetic constants were calculated using a computerized nonlinear least-squares curve-fitting program for the Macintosh, KaleidaGraph 3.0 (*1*). The purified enzyme allowed us to directly calculate the k_{cat} value based on the specific activity of each purified form of Hex B at V_{max}, assuming a M_r of 130 000.

Determination of the pH Optima of Wild-Type and E^{355}Q Hex B. Hex assay buffer normally consisting of 0.2 M Na_2HPO_4 and 0.1 M citric acid (pH 4.2) was titrated to pH 4.0, 3.5, 3.0, and 2.5 with 1 M HCl or pH 4.5, 5.0, and 5.5 with 1 M NaOH. The Hex activity was measured (*13*) at each 0.5 pH unit increment with either 0.4 μg total of Tay-Sachs fibroblast lysate protein or 2 μg of purified E^{355}Q pro-Hex B−His6. Experimental points were fitted to a 4th order polynomial equation using KaleidaGraph 3.0.

CNAG Affinity Binding Assay. The affinity ligand CNAG was synthesized and chemically coupled to Sephacryl S-200 according to Mahuran and Lowden (*24*). The ligand beads (0.3 mL) were pretreated with Hex-free 0.1% RNase A overnight to block nonspecific sites. These beads were washed with 20 mM phosphate/10 mM citrate buffer (pH 4.2) to remove residual RNase A and packed in a mini-column. Fifteen micrograms of each purified Hex protein was loaded onto individual columns. After washing twice with 2 mL of 10 mM sodium phosphate buffer, pH 6.0, containing 0.2 M NaCl (wash buffer), the specifically bound Hex protein was eluted with 150 μM δ-lactone (a competitive inhibitor) in the same wash buffer. The Hex binding affinity was calculated on the basis of the total eluted protein versus the total protein loaded on the column as determined by the Lowry method (*21*).

RESULTS

To determine the roles of the conserved acidic residues of Hex B that align with active-site residues in chitobiase (Table 1) conservative substitutions (Asp→Asn or Glu→Gln) were made at each site (Table 2). In addition, a 3′-sequence encoding a "factor Xa-His$_6$" tag was added to each mutant cDNA to facilitate the purification of the translated protein. These mutant constructs were then permanently transfected into CHO cells. Western blot analysis (Figure 2) of their cell lysates indicated that all the mutant constructs but one, βAsp^{196}Asn, produced mature (lysosomal) β-CRM, at a level similar to that of the wild-type β construct. In cells expressing the βAsp^{196}Asn construct, only precursor β-chain was detected intracellularly, indicating that this mutant protein cannot exit the ER (*22*). To confirm that the His$_6$ tag in the βAsp^{196}Asn had no effect on the processing of the mutant protein, a cDNA containing βAsp^{196}Asn alone was transfected into CHO cells. Western blot analysis revealed the identical result, i.e., detecting only precursor β-chain in the cell lysates (data not shown). Thus, the βAsp^{196}Asn substitution affects protein transport and/or folding. Consequently, we focused our subsequent experiments on the other mutants.

Since the C-terminal His$_6$-tag on the Hex B dimer does not survive the normal lysosomal environment (*18*), the

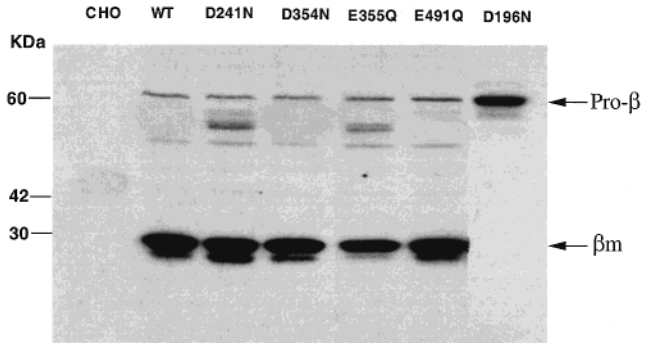

FIGURE 2: Western blot analysis using an anti-human Hex B IgG of lysates from either nontransfected CHO cells (CHO), CHO cells transfected with pcDNA-β-His$_6$ (WT) or mutant pcDNA-β*-His$_6$ encoding one of the following substitutions: Asp^{196}Asn, D196N; Asp^{241}Asn, D241N; Asp^{354}Asn, D354N; Glu^{355}Gln, E355Q; or Glu^{491}Gln, E491Q. Equal amounts of total proteins (20 μg) from each lysate were loaded. The positions corresponding to the proβ (65 kDa) and mature β (28 kDa) chains are indicated on the right. Protein standards are shown on the left.

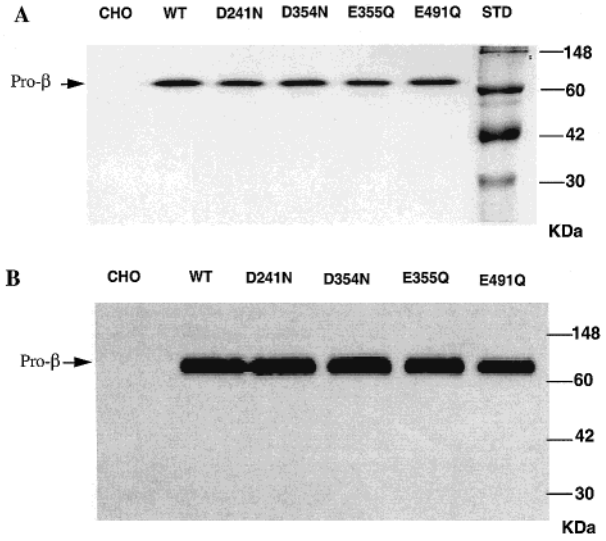

FIGURE 3: SDS−PAGE separations of Ni-NTA-purified proteins from the serum free medium of CHO cells (CHO), CHO cells transfected with pcDNA-β-His$_6$ (WT) or mutant pcDNA-β*-His$_6$ constructs. The mutant constructs encoded a Asp^{241}Asn, D241N; Asp^{354}Asn, D354N; Glu^{355}Gln, E355Q; or Glu^{491}Gln, E491Q substitution. (A) Coomassie blue staining and (B) Western blot using an anti-Hex B IgG of equal amounts of purified protein; for panel A, 4 μg in each lane, and for panel B, 0.1 μg in each lane. The M_r standard and pro-β location are indicated.

various mutant pro-Hex B−His$_6$ isozymes were isolated from the media of transfected CHO cells by Ni^{2+}-column chromatography. The complete removal of the CHO endogenous Hex and/or any small amounts of intra-species dimers was accomplished by washing with 100 mM imidazole. Analysis by SDS−PAGE produced single Coomassie-stained bands with the expected M_r of 65 000 for both the purified wild-type and mutant proteins (Figure 3A). This 65 kDa polypeptide was conclusively shown to be the β subunit of Hex by Western blot analysis with rabbit anti-human Hex B IgG (Figure 3B). No comparable polypeptide was found in the medium from the untransfected CHO cells (Figure 3B).

The access to microgram quantities of purified Hex protein enabled us to directly calculate the specific activity at 1.6 mM MUG [standard assay conditions (*13*)] of the wild type and each mutant Hex B. The mutation that made the largest

Table 3: Determination of Kinetic and CNAG-Binding Parameters for Various Forms of Hex B

Pro-Hex B-His_6	SA[a] (nmol/h/ng)	K_m (mM)[b]	V_{max} (% of WT)[b]	$k_{cat} \times 10^{-3}$[c]	$k_{cat} \times 10^{-3}/K_m$[d]	% CNAG binding[e]
mature (WT)[f]	10.1± 0.5	0.69± 0.09		1900± 200	2800± 700	75± 5
WT[f]	13.8± 0.8	0.66± 0.07	100%	2500± 300	3900± 900	71± 4
Arg211Lys[f]	0.007± 0.0004	~8	0.2%	5	0.6	7± 1
Asp240Asn[g]	1.1	~8	10%	~250	~30	ND[h]
Asp290Asn[g]	5.1	1.9± 0.2	70%	~1700	~900	ND
Asp241Asn	0.48± 0.03	1.9± 0.1	5.4%	135± 5	71± 7	7± 1
Asp354Asn	0.0057± 0.0005	0.68± 0.04	0.042%	1.1± 0.1	1.6± 0.3	68± 5
Glu355Gln	0.0029± 0.0005	0.45± 0.05	0.021%	0.52± 0.08	1.2± 0.3	76± 4
Glu491Gln	9.8± 0.8	0.69± 0.08	72%	1800± 300	2600± 800	70± 4

[a] Specific activity [under standard assay conditions (*13*)] at 1.6 mM MUG: ±SD from three independent experiments. [b] K_m (mM MUG) and % of wild-type V_{max} values (nmol MU/h/ng) ± standard errors calculated by model fitting to the Michaelis−Menten equation. [c] Maximum moles of MU released per hour per mol of purified Hex B protein (M_r 130 000). [d] Represents the rate constant for the first irreversible step in hydrolysis, likely the formation of the oxazolinium−ion intermediate. [e] Percent of Hex protein bound and specifically eluted from CNAG affinity minicolumns; ±SD from three independent experiments. [f] Data from (*18*); the wild-type mature (WT) Hex B was isolated from human placenta and contains no His_6 tag. [g] Data from Tse et al. (*19*), only the % of WT V_{max} was reported, thus k_{cat} values were approximated; these mutant proteins were not purified. [h] ND, not determined.

change in the specific activity of Hex B was the Glu^{355}Gln substitution, lowering it almost 5000-fold as compared to the wild-type value (Table 3, column 1). The Asp^{354}Asn substitution produced a Hex B with the second lowest specific activity, ~2500-fold lower. Whereas Asp^{241}Asn reduced the specific activity of Hex B ~30-fold, the Glu^{491}-Gln substitution produced a specific activity similar to the wild-type enzyme (Table 3, column 1).

We next determined the Michaelis−Menten parameters for the purified normal and each of the mutant enzymes using the MUG substrate. As previously reported, the pro-Hex B−His_6, purified from the transfected CHO cells, displayed K_m and k_{cat} values nearly identical to those determined for purified placental Hex B (Table 3) (*18*). The Glu^{491}Gln substitution had virtually no effect on the enzyme's kinetics. Thus this residue does not appear to have any role in substrate binding or catalysis in the human isozyme. When βGlu^{355}, which aligns with the catalytic acid group of chitobiase, was substituted with a Gln, the Hex B produced had a slightly decreased K_m value; however, the k_{cat} value was decreased by ~5000-fold (Figure 4, Table 3). Similar data were obtained from the βAsp^{354}Asn substitution which generated a Hex B with a normal K_m but greatly reduced, ~2000-fold, k_{cat} for MUG (Figure 4, Table 3). The aligned residue in chitobiase was a candidate for the carboxylate group that interacts with the acetamido-group of the substrate, stabilizing the transition state leading to the formation of the oxazolinium-ion intermediate. On the other hand, analysis of kinetic parameters of the Asp^{241}Asn mutant revealed a ~3-fold increase in K_m (Figure 4, Table 3) and a k_{cat} value reduced ~20-fold. Thus, βAsp^{241} is likely indirectly involved both in substrate binding and catalysis.

Further conformation of the catalytic role of βGlu^{355} was obtained by examining the pH optimum of the βGlu^{355}Gln mutant. The pH optimum was shifted by about −0.7 pH units to pH 3.5 (Figure 5).

We have recently shown that CNAG binding can be used as an assay to differentiate the effect of a mutation on substrate binding versus catalysis (*18*). To confirm the kinetically defined roles of the above residues, 15 μg of purified normal or mutant protein was loaded on a CNAG affinity minicolumn. The Asp^{354}Asn, Glu^{355}Gln and Glu^{491}-Gln mutants, all of which hydrolyze MUG with near normal

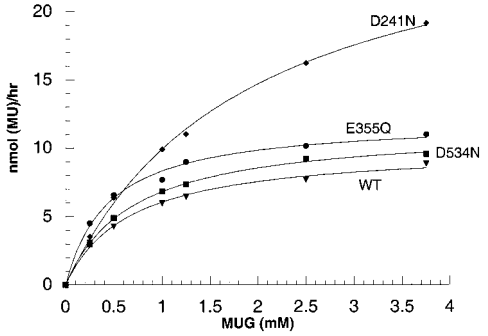

FIGURE 4: Kinetic analysis of wild-type pro-Hex B-His_6 (WT) and three mutant pro-Hex B*-His_6 using the neutral MUG (mM) substrate. The amount of purified normal (0.51 ng) and mutant Hex proteins (27−3000 ng) used was optimized for each construct such that levels of Hex activity were obtained that could be measured accurately. The mutations include Asp^{241}Asn, D241N (27 ng); Asp^{354}Asn, D354N (1400 ng); and Glu^{355}Gln, E355Q (3000 ng). Hex B containing a Glu^{491}Gln substitution is not shown as it produced kinetic data nearly identical to those of the wild type control. The actual experimental data points are shown, which were directly fitted to the Michaelis−Menten equation. The equation with its calculated best-fit constants (K_m and apparent V_{max}) were then used to generate the curve that overlays the data points on the graph. The R values for all of the experiments were >0.995. The actual K_m and V_{max} values are given in Table 3.

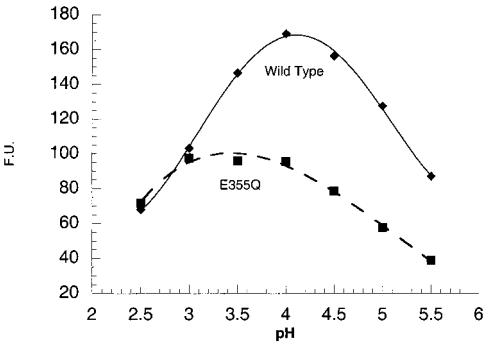

FIGURE 5: pH optima of the wild-type Hex B and the E^{355}Q mutant Hex B, "Fl. Units" are arbitrary fluorescent units (minus substrate blanks). The actual experimental data points are shown, which were directly fitted to a fourth order polymonial equation. The R values for each experiment were >0.99.

K_m values, also exhibited approximately the same level of binding affinity as either the wild-type enzyme or purified placental Hex B. By comparison, the replacement of Asp^{241}

with Asn produced a Hex B with a much lower binding capacity, 7%, relative to the wild-type enzyme, consistent with its higher observed K_m value (Table 3, columns 3 and 9).

DISCUSSION

We have previously shown that some evolutionarily conserved acidic residues are involved in the active sites of the human Hex subunits (*19*). Recently, molecular modeling of human Hex from the structure of chitobiase predicts that there are eight conserved active-site Asp or Glu residues (Table 1). Among these, Asp^{208}, Asp^{240}, and Asp^{290} in Hex B have been partially characterized (*19*). In this early study, the mutant proteins were not fully purified and the signal (human Hex) to noise (endogenous Hex) ratio after human-specific immunoprecipitation was ~100:1; thus, the values obtained from this approach must be considered only approximate. One apparently incorrect conclusion made in the study was that βAsp^{196} was an active-site residue involved in catalysis. Since this residue is not predicted by the chitobiase model to be in the active site, we reexamined the original Asp^{196}Asn mutant (with and without the added His$_6$-tag) and were unable to detect any mature β chains (precursor β was present) in permanently transfected CHO cells. Nucleotide sequencing confirmed the presence of the single missense mutation in the βcDNA (data not shown). Thus, this residue is required for intracellular transport. We are unable to explain the previously reported observation of normal levels of mature β chain in transfected cells. We also found that substitution of βAsp^{208} with Asn produced only monomeric precursor β chains (*19*). In another recent study we confirmed that the βAsp^{208}Asn mutant protein was trapped in the ER (*22*). The Asp^{240}Asn mutant had no effect on intracellular transport, but was shown to have a higher K_m than the wild-type enzyme and a 10-fold lower V_{max}. The βAsp^{290}Asn substitution interfered with intracellular transport (~20-fold reduction in mature β chains from wild-type levels) increased the K_m for MUG by ~3-fold and slightly reduced (70% of wild type) the isozyme's V_{max} value (the significance of such a small change is questionable). Thus, Asp^{208} and possibly Asp^{196} are critical for formation of the dimer, which is required for intracellular transport (*25*); Asp^{240} is involved in both substrate binding and catalysis; and Asp^{290} is needed to induce efficient intracellular transport, substrate binding, and may also play a small role in catalysis.

The above data for Asp^{240} and Asp^{290} are consistent with the molecular modeling of human Hex based on the chitobiase structure (c-Asp^{378} and Asp^{448}) (Table 1) (*8*). The suggestion that βAsp^{290} may play a role in catalysis, as well as substrate binding, was supported experimentally in a recent study of Sp-Hex (*9*). Modeling of this enzyme from the chitobiase structure indicated that Sp-Asp^{246} aligns with c-Asp^{448} which aligns with human βAsp^{290} (Table 1). When Sp-Asp^{246} was converted to Asn and the enzyme purified from transformed *Escherichia coli*, its K_m was increased and its specific activity at V_{max} decreased by ~2-fold. The chitobiase model suggests that this residue facilitates substrate-binding through an indirect hydrogen bond via a bound water molecule, and may be involved in catalysis through a hydrogen bond with another acidic active-site residue, c-Asp^{539} (βAsp^{354} or SpAsp^{539}, see below).

In the present study, we examined the role(s) of the other four candidate active acidic amino acids using our recently developed His$_6$-tagging procedure that results in a very high signal-to-noise ratio (~50000:1) (*18*). Using this procedure, we have demonstrated that βArg^{211}, which aligns with αArg^{178} (the residue substituted in classical B1-variant of Tay-Sachs disease), plays an essential role in both substrate binding and catalysis (Table 1). Although no role in catalysis was assigned by the authors of the chitobiase model to the residue that aligns with βArg^{211}, c-Arg^{349}, we found that a βArg^{211}Lys substitution raised K_m 10-fold and reduced k_{cat} by 500-fold (0.2% of wt) (*18*). Substitution of the aligned Arg in Sp-Hex for His resulted in a 40-fold increase in K_m and a 5-fold reduction in V_{max} (*9*). Thus, while both sets of experimental data agree that this Arg residue is important for both substrate binding and catalysis, the degrees of its importance appear to vary between the isozymes.

It is difficult to assign distinct roles to active-site residues based on a single three-dimensional structure. Although residues such as c-Arg^{349} may appear to be at good distances for forming hydrogen bonds with the substrate molecule, they may be at even more advantageous positions to stabilize the transition state thereby assisting in catalysis as well as substrate binding. Indeed such a role for c-Arg^{349} is suggested in the chitobiase model as the nonreducing NAG-A (GlcNAc) was found to be bound to this residue in a distorted, apparently energetically unfavorable 4-sofa conformation (*8*). Such a progression from loosely bound substrate to tightly bound transition state as part of the catalytic mechanism has been documented in other enzymes for which there are more extensive crystallographic analyses (*26*−*28*).

In chitobiase, the critical Arg^{349} is held in place by polar interactions with four other residues; the terminal amino and imino groups hydrogen bond to c-Asp^{346}, c-Asp^{378}, and a water molecule coordinated by c-Asp^{379} and c-Glu^{380} (*8*). In human Hex B, these residues appear not to be conserved. c-Asp^{346} aligns with βAsp^{208}, which in the human isozyme is involved in dimer formation. c-Glu^{380} is not conserved at all, aligning with βGln^{242} and αPro^{209} (Table 1). This leaves only βAsp^{240} (c-Asp^{378}) and βAsp^{241} (c-Asp^{379}) to hold βArg^{211} in place. Thus, the chitobiase model predicts that the function of βAsp^{240} and βAsp^{241} is to orient βArg^{211} for its role in binding and catalysis. Our experimental data support this because a conservative substitution of either of these Asp residues also causes both an increase in K_m and a decrease in the k_{cat} (Table 3).

The conventional acid−base catalytic mechanism for many glycosidases relies heavily on both a catalytic acid/base group and a catalytic nucleophile, e.g., an unprotonated Asp or Glu (*29*). In chitobiase (*8*) and presumably human Hex (*7*), the role of the catalytic nucleophile is played by the neighboring C-2 acetamido group, leading to a cyclic oxazolinium-ion intermediate, rather that the conventional covalent glycosyl−enzyme intermediate. However, formation of the cyclic oxazolinium-ion intermediate is itself assisted by another carboxylate in the active site that interacts with the nitrogen of the *N*-acetyl group on the substrate. This residue presumably functions to stabilize the transition state leading to the formation of the intermediate by dispersing the developing positive charge on the oxazolinium-ion ring. One of the strongest candidates for this group in chitobiase is the unprotonated c-Asp^{539} residue, which aligns with βAsp^{354}.

When we converted βAsp[354] to Asn, we produced a mutant protein with the second lowest k_{cat} we have observed, only 0.04% of the wt value, but with an apparently normal K_m (Table 3). These data are consistent with the role proposed for c-Asp[539] on the basis of the crystal structure of the chitobiase substrate complex. An Asp[539]Ala mutation of this residue in the chitobiase enzyme revealed a markedly different effect on the kinetic parameters. In that study, K_m decreased by approximately 30-fold while k_{cat} decreased 50-fold. A direct comparison of these results with those obtained in this study is of questionable value as the mutations made in each case are quite different (an Asp[539]Asn substituted chitobiase was not expressed). However, a crystal structure of the Ala mutant in complex with chitobiose revealed that this residue was indeed critical for orienting the acetamido group for catalysis (*30*).

The catalytic acid−base group in chitobiase is predicted to be c-Glu[540] (*8*), which aligns with βGlu[355] and αGlu[323] (Table 1). Three previous reports have linked both the aligned α and β residues to the active site of human Hex. However, none have conclusively shown either Glu to be the catalytic acid/base group because of the low signal-to-noise ratios of the isolated proteins, <100:1, and thus their inability to ensure that kinetic data were not from contaminating endogenous enzyme.

In the first report made prior to the publication of the chitobiase model, βGlu[355] was identified through its reaction with a photoaffinity label and initially predicted to be involved in substrate binding (*31*). However, no mutational studies were reported to substantiate this prediction.

With knowledge of the chitobiase model, an αGlu[323]Asp-substituted Hex A (aligns with βGlu[355], Table 1) was expressed in a human fetal Tay-Sachs disease neuroglial (TSD-NG) cell line (*16*). This method relies on the recruitment of an endogenous human β subunit by the transfected human mutant α for the production and purification of Hex A, followed by kinetic analysis using α-specific MUGS. Thus, the signal-to-noise ratio, ∼75:1, in this study was limited by the residual activity of Hex A's normal β subunit toward MUGS [MUG:MUGS ∼300:1 for Hex B and 4:1 for Hex A (*1*)]. This study provided the first direct evidence that βGlu[355] and by extension αGlu[323] are part of the active sites of human Hex.

Finally, with knowledge of the chitobiase model and based on data obtained through mutational analysis and baculovirus/insect cell expression by the same group that developed the photoaffinity label (see above), it was concluded that βGlu[355] is involved in catalysis, rather than substrate binding (*17*). The βGlu[355] mutant proteins had an apparently normal K_m, but a reduced V_{max} value, i.e., near the background level of the untransfected cell. In this study the mutant human Hex Bs and the endogenous insect cells' Hex B were co-purified resulting in a signal-to-noise ratio of only ∼20:1. As well, because of the low levels of protein recovered from their affinity column, V_{max} values had a stated experimental error of ∼50%. Thus, the authors were unable to conclusively attribute the apparently normal K_m they obtained to the mutant human Hex Bs, rather than to the contaminating endogenous insect cell Hex (*17*). This is the same problem that we encountered with our initial kinetic analyses of the βArg[211]Lys mutation, expressed in COS cells and purified by immuno-precipitation (signal-to-noise of ∼75:1), that resulted in an apparently normal K_m for the mutant enzyme with a V_{max} reduced to background levels (*14*).

Thus, despite three independent studies, no previous experimental data have obtained a signal-to-noise ratio sufficient to identify βGlu[355] or αGlu[323] as the catalytic acid−base groups in human Hex.

Additionally, a Glu[540]Ala chitobiase mutant showed only a decrease of 140-fold in k_{cat} and a 4-fold decrease in K_m relative to the wild-type enzyme (*30*). In Sp-Hex the residue that aligns with c-Glu[540] is Glu[314] (Table 1) and when this residue was mutated to Gln there was a 7-fold decrease in K_m and a 300-fold decrease in V_{max} (*9*). While the results obtained with these two prokaryotic enzymes agree well with each other the reduction in k_{cat} is less than normally would be expected from an enzyme whose catalytic acid group had been neutralized (*15*, *32*).

Our data on the βGlu[355]Gln substituted human Hex B are totally consistent with this residue functioning as the catalytic acid. While the k_{cat} was reduced to the lowest level of any mutant Hex so far generated, 0.02% of the wt value, the K_m of the mutant enzyme was slightly decreased, i.e., did not correspond to the K_m of the normal human isozyme or the endogenous CHO Hex B (Table 3). As well, like the wild-type Hex B and those other mutant forms with normal values of K_m, ∼70% of the βGlu[355]Gln Hex B protein bound to and was specifically eluted from the Hex-affinity column, despite its lack of catalytic activity (Table 3). Finally, we found a shift in the mutant's pH optimum of about −0.7 pH units (Figure 5), consistent with its role in catalysis and again confirming that we were not examining low levels of endogenous CHO enzyme. As with our other Hex mutations, proper folding was indirectly assured by the uninhibited passage of the protein through the ER's quality control system (*18*, *20*, *22*) (Figure 2).

The most C-terminal residue we analyzed was βGlu[491], which we substituted with Gln. The mutant Hex B produced had kinetic parameters nearly identical to those of the wild-type enzyme (Table 3). The βGlu[491] aligns with c-Glu[739]. The chitobiase structure revealed that this residue participates along with the substrate's aglycan 5-OH (NAG-B) in binding a molecule of water. This water molecule has been predicted to be the incoming water that attacks the anomeric center, with assistance from the general acid/base catalytic residue (Glu[314] in chitobiase and βGlu[355] in human β-hexosaminidase), to effect the hydrolysis of the oxazolinium-ion intermediate. These data would suggest that the human βGlu[491] may be an important active-site residue. However, since there is no binding site in human Hex for the aglycan, which corresponds to the NAG-B group in chitobiase substrate, it is not that surprising that this residue does not have a vital function in the human isozymes. Additionally, this residue is not conserved in Sp-Hex (Table 1).

Our mutational examination of the candidate active-site residues in human Hex thus far is concordant with the roles predicted from the chitobiase molecular model. Therefore the active-site structure modeled for human Hex and its associated substrate assisted mechanism for catalysis appears to be generally valid, indicating that human Hex and probably all the Family 20 enzymes have similar structures and catalytic mechanisms. However, the present model is not sufficient to fully understand the structure−function relationships in human Hex, particularly its requirement for dimer-

ization and interaction with the GM2 ganglioside/GM2 activator protein complex. Nor is the present model sufficient to predict the degree to which a missense mutation will alter the folding patterns of the protein and affect intracellular transport. Thus, three-dimensional structures of a human isozyme with and without a bound ligand are still needed before geneotype−phenotype correlations can be predicted.

REFERENCES

1. Hou, Y., Tse, R., and Mahuran, D. J. (1996) *Biochemistry 35*, 3963−3969.
2. Mahuran, D. J. (1998) *Biochim. Biophys. Acta 1393*, 1−18.
3. Gravel, R. A., Clarke, J. T. R., Kaback, M. M., Mahuran, D., Sandhoff, K., and Suzuki, K. (1995) in *The Metabolic and Molecular Bases of Inherited Disease* (Scriver, C. R., Beaudet, A. L., Sly, W. S., and Valle, D., Eds.) pp 2839−2879, McGraw-Hill, New York.
4. Mahuran, D. J. (1999) *Biochim. Biophys. Acta 1455*, 105−138.
5. Henrissat, B. (1991) *Biochem. J. 280*, 309−316.
6. Legler, G., and Bollhagen, R. (1992) *Carbohydr. Res. 233*, 113−123.
7. Knapp, S., Vocadlo, D., Gao, Z. N., Kirk, B., Lou, J. P., and Withers, S. G. (1996) *J. Am. Chem. Soc. 118*, 6804−6805.
8. Tews, I., Perrakis, A., Oppenheim, A., Dauter, Z., Wilson, K. S., and Vorgias, C. E. (1996) *Nat. Struct. Biol. 3*, 638−648.
9. Mark, B. L., Wasney, G. A., Salo, T. J. S., Khan, A. R., Cao, Z. M., Robbins, P. W., James, M. N. G., and Triggs-Raine, B. L. (1998) *J. Biol. Chem. 273*, 19618−19624.
10. Mahuran, D. J. (1997) in *Protein Dysfunction in Human Genetic Disease* (Swallow, D., and Edwards, Y., Eds.) pp 99−117, Bios Scientific, Oxford U.K.
11. Kytzia, H. J., Hinrichs, U., Maire, I., Suzuki, K., and Sandhoff, K. (1983) *EMBO J. 2*, 1201−1205.
12. Ohno, K., and Suzuki, K. (1988) *J. Neurochem. 50*, 316−318.
13. Brown, C. A., Neote, K., Leung, A., Gravel, R. A., and Mahuran, D. J. (1989) *J. Biol. Chem. 264*, 21705−21710.
14. Brown, C. A., and Mahuran, D. J. (1991) *J. Biol. Chem. 266*, 15855−15862.
15. Ly, H. D., and Withers, S. G. (1999) *Annu. Rev. Biochem. 68*, 487−522
16. Fernandes, M. J. G., Yew, S., Leclerc, D., Henrissat, B., Vorgias, C. E., Gravel, R. A., Hechtman, P., and Kaplan, F. (1997) *J. Biol. Chem. 272*, 814−820.
17. Pennybacker, M., Schuette, C. G., Liessem, B., Hepbildikler, S. T., Kopetka, J. A., Ellis, M. R., Myerowitz, R., Sandhoff, K., and Proia, R. L. (1997) *J. Biol. Chem. 272*, 8002−8006.
18. Hou, Y., Vocadlo, D., Withers, S., and Mahuran, D. (2000) *Biochemistry 39*, 6219−6227.
19. Tse, R., Vavougios, G., Hou, Y., and Mahuran, D. J. (1996) *Biochemistry 35*, 7599−7607.
20. Hou, Y., Vavougios, G., Hinek, A., Wu, K. K., Hechtman, P., Kaplan, F., and Mahuran, D. J. (1996) *Am. J. Hum. Genet. 59*, 52−58.
21. Lowry, O. H., Rosebrough, N. J., Farr, A. L., and Randall, R. J. (1951) *J. Biol. Chem. 193*, 265−275.
22. Hou, Y., McInnes, B., Hinek, A., Karpati, G., and Mahuran, D. (1998) *J. Biol. Chem. 273*, 21386−21392.
23. Brown, C. A., and Mahuran, D. J. (1993) *Am. J. Hum. Genet. 53*, 497−508.
24. Mahuran, D. J., and Lowden, J. A. (1980) *Can. J. Biochem. 58*, 287−294.
25. Proia, R. L., d'Azzo, A., and Neufeld, F. (1984) *J. Biol. Chem. 259*, 3350−3354.
26. Uitdehaag, J. C., Mosi, R., Kalk, K. H., van der Veen, A., Dijkhuisen, L., Withers, S. G., and Dijkstra, B. (1999) *Nat. Struct. Biol. 6*, 432−436.
27. Davies, G. J., Mackenzie, L., Varrot, A., Dauter, M., Brzozowski, A. M., Schulein, M., and Withers, S. G. (1998) *Biochemistry 37*, 11707−11713.
28. Sidhu, G., Withers, S. G., Nguyen, N. T., McIntosh, L. P., Ziser, L., and Brayer, G. D. (1999) *Bichemistry 38*, 5346−5354.
29. Withers, S. G., Rupitz, K., Trimbur, D., Antony, R., and Warren, A. J. (1992) *Biochemistry 31*, 9979−9985.
30. Prag, G., Papanikolau, Y., Tavlas, G., Vorgias, C. E., Petratos, K., and Oppenheim, A. B. (2000) *J. Mol. Biol. 300*, 611−617.
31. Liessem, B., Glombitza, G. J., Knoll, F., Lehmann, J., Kellermann, J., Lottspeich, F., and Sandhoff, K. (1995) *J. Biol. Chem. 270*, 23693−23699.
32. MacLeod, A. M., Lindhorst, T., Withers, S. G., and Warren, R. A., J,. (1994) *Biochemistry 33*, 6371−6376.

BI002018S